ICANS-XIV
14th Meeting of the International Collaboration on
Advanced Neutron Sources
June 14-19, 1998
Starved Rock Lodge, Utica, Illinois, USA

General Time-Focusing of the Pulsed-Source Crystal Analyzer Spectrometer*

J. M. Carpenter
Intense Pulsed Neutron Source
Argonne National Laboratory

ABSTRACT

This paper outlines the derivation of an expression for the resolution of a crystal analyzer spectrometer and gives explicit conditions for geometric focusing. The development preserves full 3-dimensional generality so as to guide the choice of geometric parameters in the design of instruments. Historically, the high-resolution crystal analyzers are "backscattering" instruments, for which the Bragg angle is close to 90 degrees. The present results indicate that comparable high resolution can be attained using more general analyzer angles, which may provide some advantageous options for design. The focusing relationships define continuous, focused surfaces, and the results also provide a way to assess the resolution of a spectrometer built up of small, focused planar elements.

1. PRELIMINARY ANALYSIS

Figure 1 shows the conceptual layout of a crystal analyzer spectrometer. Pulses of neutrons emerge from the moderator surface "m" having wavelength λ'. Neutrons strike a sample "s" where they are scattered inelastically with energy gain ε to wavelength λ. Scattered neutrons impinge on the analyzer crystal "x" where, if their wavelength and incident angle are appropriate, they scatter, and if scattered in the appropriate direction, register in the detector "d".

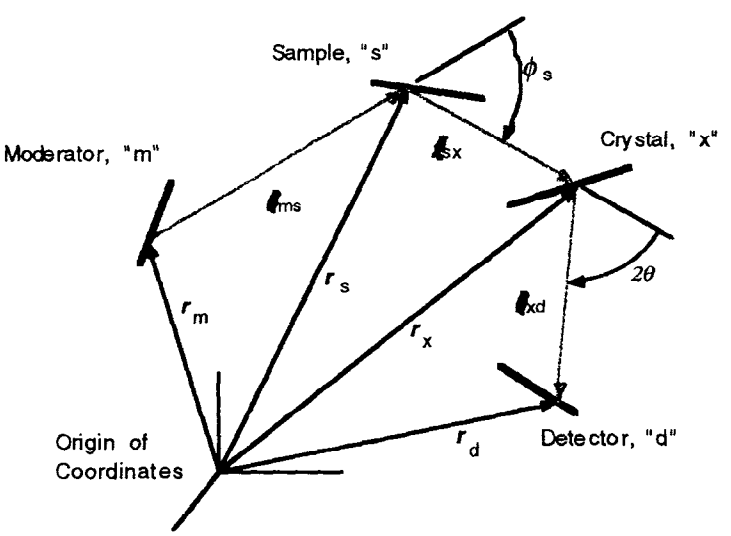

Figure 1. Schematic diagram of a crystal analyzer spectrometer. The figure shows a general neutron trajectory through the instrument (red). The elements m, s, x, and d (blue) are two-dimensional surfaces in a general, three-dimensional, non-planar arrangement.

* This work was performed under U. S. Government contract No. W-31-109-ENG-38.

We treat the instrument as having a thin sample, a thin analyzer crystal, and a thin detector, all planar. The angular distribution of neutrons from the source is isotropic and we ignore angular variation of the scattering and detection probabilities. There are no collimators.

The time to fly from the moderator surface to the detector is

$$t = \ell_1/v' + (\ell_2 + \ell_3)/v \,, \tag{1}$$

where v' and v are the neutron speeds before and after scattering, and ℓ_1, ℓ_2 and ℓ_3 are the distances between general points $\boldsymbol{r}_m$, $\boldsymbol{r}_s$, $\boldsymbol{r}_x$ and $\boldsymbol{r}_d$ on the moderator, sample, analyzer crystal, and detector surfaces, respectively. We seek to describe the instrument response when the scattering energy gain ε is unique,

$$\varepsilon = \frac{h^2}{2m}\left(1/\lambda'^2 - 1/\lambda^2\right) . \tag{2}$$

Then the flight time is

$$t = \frac{m}{h}(\ell_1\lambda' + (\ell_2 + \ell_3)\lambda) \,, \tag{3}$$

where

$$\lambda = \frac{h}{mv} \,. \tag{4}$$

2. FLIGHT PATH LENGTHS AND TIME OF FLIGHT

We pursue an analysis linearized in the small deviations of quantities from their mean values. While there are a number of equivalent ways to go about it, we develop an expression for the flight time, term by term and factor by factor, using expansions to first order in the deviations to arrive finally at a result which is linear in the deviations. This approach has the advantage of transparency, albeit at the expense of length.

We express the lengths of flight paths in terms of mean values and deviations from the mean values,

$$\ell_1 = \ell_1(\boldsymbol{r}_m,\boldsymbol{r}_s) = L_1 + \delta\ell_1(\boldsymbol{r}_m,\boldsymbol{r}_s) \tag{5}$$

$$\ell_2 = \ell_2(\boldsymbol{r}_s,\boldsymbol{r}_x) = L_2 + \delta\ell_2(\boldsymbol{r}_s,\boldsymbol{r}_x) \tag{6}$$

$$\ell_3 = \ell_3(\boldsymbol{r}_x,\boldsymbol{r}_d) = L_3 + \delta\ell_3(\boldsymbol{r}_x,\boldsymbol{r}_d) \tag{7}$$

where the mean values are

$$L_1 = \left\langle \ell_1(\boldsymbol{r}_m,\boldsymbol{r}_s) \right\rangle \text{, etc.} \tag{8}$$

The averages are taken over the allowed positions on m, s, x and d. Throughout, boldface characters denote vector quantities; the circumflex designates a unit vector.

For a given path ($\boldsymbol{r}_m$, $\boldsymbol{r}_s$, $\boldsymbol{r}_x$, $\boldsymbol{r}_d$) through the instrument the analyzer scattering angle 2θ is unique, the Bragg angle is

$$\theta = \theta(\boldsymbol{r}_s,\boldsymbol{r}_x,\boldsymbol{r}_d) = \theta_o + \delta\theta(\boldsymbol{r}_s,\boldsymbol{r}_x,\boldsymbol{r}_d) \tag{9}$$

and only one wavelength λ is reflected,

$$\lambda = \lambda(r_s r_x r_d) = 2d \sin\left(\theta(r_s r_x r_d)\right), \tag{10}$$

$$\lambda = 2d \sin\theta_o(1 + \cot\theta_o \delta\theta(r_s r_x r_d)) = \lambda_o + \delta\lambda(r_s r_x r_d). \tag{11}$$

For scattering with unique energy gain ε [equation (2)] if the mean wavelength after scattering is λ_o, the mean incident wavelength is λ'_o

$$\lambda'^2_o = 1/(1/\lambda_o^2 + 2m\varepsilon/h^2) \tag{12}$$

so the ratio of pre- and post-scattering wavelengths is

$$\lambda'_o / \lambda_o = 1/\sqrt{1 + 2m\varepsilon\lambda_o^2/h^2}. \tag{13}$$

Meanwhile, with ε fixed, when λ differs from λ_o then λ' differs from λ_o' by an amount found by differentiating the relationship (2), expressed in homogeneous form,

$$F(\lambda,\lambda';\varepsilon) = 1/\lambda'^2 - 1/\lambda^2 - 2m\varepsilon/h^2 = 0, \tag{2'}$$

$$\left.\frac{\partial F}{\partial\lambda}\right|_{\lambda_o}\delta\lambda + \left.\frac{\partial F}{\partial\lambda'}\right|_{\lambda'_o}\delta\lambda' = 2/\lambda_o^3\delta\lambda - 2/\lambda'^3_o\delta\lambda' = 0 \tag{14}$$

so that

$$\delta\lambda' = (\lambda'_o/\lambda_o)^3\delta\lambda. \tag{15}$$

Then the flight time for a general neutron trajectory is

$$t = t(r_m r_s r_x r_d) = \frac{m}{h}\{(L_1 + \delta\ell_1(r_m r_s))(\lambda'_o + \delta\lambda') +$$

$$+ (L_2 + \delta\ell_2(r_s r_x) + L_3 + \delta\ell_3(r_x r_d))(\lambda_o + \delta\lambda)\} \tag{16}$$

which to first order in the deviations of the flight paths and wavelengths from the means is

$$t = \frac{m}{h}\{\lambda'_o L_1 + \lambda_o(L_2 + L_3) + \lambda'_o\delta\ell_1 + \lambda_o(\delta\ell_2 + \delta\ell_3) + L_1\delta\lambda' + (L_2 + L_3)\delta\lambda\}. \tag{17}$$

We have defined the mean values so that the deviations average to zero. The first term is the dominant term t_o,

$$t_o = \frac{m}{h}(\lambda'_o L_1 + \lambda_o(L_2 + L_3)), \tag{18}$$

which is independent of the deviations. Thus, after a few steps of algebra, in view of (11), we can express the time of flight in terms of the deviations (which depend on the path through the instrument)

$$t = t_o + \frac{1}{v_o}[(\lambda'_o/\lambda_o)\delta\ell_1 + (\delta\ell_2 + \delta\ell_3)] + \frac{1}{v_o}[(\lambda'_o/\lambda_o)^3 L_1 + (L_2 + L_3)]\cot\theta_o\delta\theta. \tag{19}$$

It turns out to be more convenient to express the wavelength deviation

$$\delta\lambda = \lambda_o \cot\theta_o \delta\theta \tag{20}$$

in terms of the deviation of $\cos 2\theta$ from its nominal value,

$$\delta\lambda = 2d\,\delta(\sin\theta) = 2d\,\frac{\partial(\sin\theta)}{\partial(\cos 2\theta)}\delta(\cos 2\theta)\,. \tag{21}$$

Since

$$\sin\theta = \sqrt{(1-\cos 2\theta)/2}\,, \tag{22}$$

$$\frac{\partial(\sin\theta)}{\partial(\cos 2\theta)} = -\frac{1}{4}\frac{1}{\sqrt{(1-\cos 2\theta)/2}} = -\frac{1}{4\sin\theta} \tag{23}$$

so that

$$\delta\lambda = -2d\left(\frac{1}{4\sin\theta_o}\right)\delta(\cos 2\theta) = -\lambda_o\delta(\cos 2\theta)/4\sin^2\theta_o\,. \tag{24}$$

Therefore the flight time for a general neutron trajectory is

$$t = t_o + \frac{1}{v_o}[(\lambda'_o/\lambda_o)\delta\ell_1 + (\delta\ell_2 + \delta\ell_3)] - \frac{1}{4v_o}[(\lambda'_o/\lambda_o)^3 L_1 + (L_2 + L_3)]\frac{1}{\sin^2\theta_o}\delta(\cos 2\theta)\,. \tag{25}$$

3. THE COUNTING RATE DISTRIBUTION

The observed counting rate distribution $C(T)$ at time T is the weighted sum of the rates for all the allowed paths through the instrument,

$$C(T) = \int i(\lambda',t')F_m(\mathbf{r}_m)F_s(\mathbf{r}_s)P_x(\mathbf{r}_x,\lambda,\hat{q})P_d(\mathbf{r}_d,\lambda)\delta(T - t' - t(\mathbf{r}_m,\mathbf{r}_s,\mathbf{r}_x,\mathbf{r}_d))\,d^2\mathbf{r}_m\,d^2\mathbf{r}_s\,d^2\mathbf{r}_x\,d^2\mathbf{r}_d\,dt' \tag{26}$$

where the wavelengths λ and λ' depend uniquely on the path through the instrument. Here, $F_m(\mathbf{r}_m)$ represents the distribution of intensity on the moderator surface and $F_s(\mathbf{r}_s)$ represents the distribution of the allowed points on the sample. We assume that the wavelength-time distribution $i(\lambda',t')$ is independent of position on the moderator surface and slowly varying with respect to wavelength, though sharply varying with time,

$$i(\lambda',t') \approx i(\lambda'_o,t')\,. \tag{27}$$

Considering that the detection probability is independent of the position of the incident neutron and (already assumed in the treatment outlined above) independent of the direction of incidence, and moreover, is slowly varying with respect to wavelength,

$$P_d(\mathbf{r}_d,\lambda) = \eta(\lambda)F_d(\mathbf{r}_d) \approx \eta(\lambda_o)F_d(\mathbf{r}_d)\,. \tag{28}$$

Equation (26) does not include an overall normalization factor accounting for, for example, the $1/r^2$ variation of the intensity or for the scattering power of the sample. Thus (26) as written (for simplicity) gives only a relative intensity, while it provides for a valid calculation of the resolution.

The probability of reflection from the crystal decomposes similarly into a product

$$P_x(\boldsymbol{r}_x,\lambda,\hat{q}) = F_x(\boldsymbol{r}_x)p_x(\lambda,\hat{q}) \approx F_x(\boldsymbol{r}_x)p_x(\lambda_o,\hat{q}) \tag{29}$$

in which $F_x(\boldsymbol{r}_x)$ represents the distribution of allowed points on the crystal, and $p_x(\lambda,\boldsymbol{q})$ is the angle-dependent reflection probability, which depends strongly on $\boldsymbol{q}$, the direction of momentum transfer of the neutron, and weakly on the wavelength, since we have already built in the Bragg condition. Figure 2 illustrates the analyzer geometry, which could be either a reflection (shown) or a transmission arrangement.

The reflection probability must account for a mosaic distribution of finite width and for secondary extinction, which flattens the reflectivity distribution. We ignore the shift in reflecting position due to propagation of neutrons in the crystal and incorporate everything else in the function $p_x(\lambda,\boldsymbol{q})$ which depends parametrically on the nominal reflecting vector τ_o , the unit vector perpendicular to the nominal reflecting planes. The 2-dimensional distribution $p_x(\lambda,\boldsymbol{q})$ (a scalar function) depends on individual crystal properties, and is sharply peaked for values of $\boldsymbol{q}$ near τ_o .

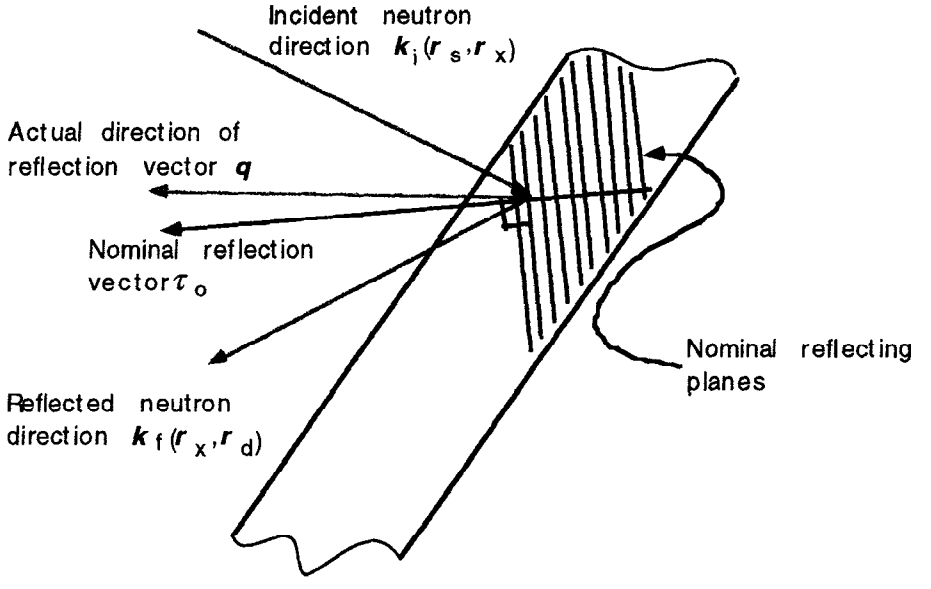

Figure 2. Diagram of crystal reflection, intentionally general in that the reflecting planes are not parallel to the cut plane of the crystal.

For the moment we denote the reflection probability as a function of the vector $\boldsymbol{q}\times\tau_o$, a measure of the deviation of $\boldsymbol{q}$ from τ_o

$$p_x(\lambda_o,\hat{q}) = f_x(\lambda_o,\hat{q}\times\hat{\tau}_o) , \tag{30}$$

which is a function similar to that shown in Figure 3.

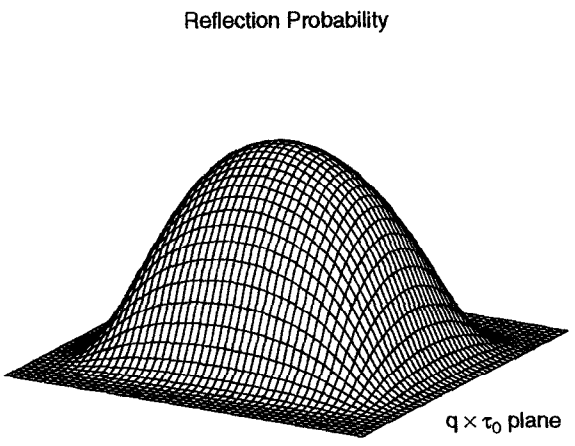

Figure 3. Schematic illustration of the reflection probability function.

The angular distribution of neutrons reflected by the analyzer crystal, and thus the spectrometer resolution in the absence of focusing, is doubly determined: by the strictly geometric effects of the finite sample, analyzer crystal, and detector; and by the effect of the mosaicity and orientation of the reflecting planes of the crystal.

4. OUTLINE OF THE FOCUSING CALCULATION

Now we clarify the intent of our effort. We compute the counting rate function C(T) (which applies for the given, fixed energy transfer ε),

$$C = \int C(T)dT \tag{31}$$

$$\bar{T} = \frac{1}{C}\int T\, C(T)dT \tag{32}$$

$$\sigma_T^2 = \frac{1}{C}\int (T-\bar{T})^2 C(T)dT \tag{33}$$

Focusing implies that σ_T^2 is a minimum with respect to instrument parameters.

It is of central importance to treat the expression for the counting rate function C(T) in terms of distributions of independently distributed variables; these appear in the overall distribution as products of distributions of individual variables. Thus it would be incorrect to compute σ_T^2 using expression (19) assuming, for example, that $\delta\ell_1$ is independent of $\delta\ell_2$ and $\delta\theta$; the independently distributed variables are r_m, r_s, r_x, r_d. Both $\delta\ell_1$ and $\delta\ell_2$ depend, for example, on r_s, so variations in $\delta\ell_2$ are not independent of variations in $\delta\ell_1$. Therefore we must eventually reduce our expression for the time of flight, t, to one that depends explicitly on the independently distributed variables.

First, however, we note a simplifying feature of the problem, namely that the emission time distribution, at least within our approximation, only broadens the overall result and does not require separate analysis. Writing (26) as

$$C(T) = \int i(\lambda'_o, t')\delta(T - t' - \tau)c(\tau)dt'd\tau \tag{34}$$

where

$$c(\tau) = \int F_m(\mathbf{r}_m) F_s(\mathbf{r}_s) F_x(\mathbf{r}_x) p_x(\bar{q}(\mathbf{r}_s, \mathbf{r}_x, \mathbf{r}_d)) F_d(\mathbf{r}_d) \eta(\lambda_o) \times$$

$$\times \delta(\tau - t(\mathbf{r}_m, \mathbf{r}_s, \mathbf{r}_x, \mathbf{r}_d))\, d^2\mathbf{r}_m\, d^2\mathbf{r}_s\, d^2\mathbf{r}_x\, d^2\mathbf{r}_d \tag{35}$$

we find that the mean time of the counting rate distribution is

$$\bar{T} = \bar{T}_i(\lambda'_o) + t_o \tag{36}$$

in which $\bar{T}_i(\lambda'_o)$ is the mean of the pulse emission time distribution for neutrons of wavelength λ'_o, and the variance of the counting time distribution is

$$\sigma_T^2 = \sigma_i^2(\lambda'_o) + \sigma_g^2(\lambda_o)\,. \tag{37}$$

Here t_o is the mean flight time through the instrument. σ_g^2 is the time variance due to the instrument geometry alone, which is the object of our consideration and is to be minimized while the counting rate C is made maximum. $\sigma_i^2(\lambda'_o)$ is the variance of the emission time distribution which is a quantity determined by the moderator properties. We will ignore effects of the source pulse emission time distribution in the work immediately to follow. However, the width of the emission time distribution imposes an irreducible lower limit on the resolution of the instrument and sets the scale for the geometric resolution.

5. EXPRESSIONS FOR DISTANCES AND ANGLES

Now we must obtain explicit expressions for the distances, angles, etc., and the deviations of these from their mean values, in terms of the independently distributed variables, the positions $\mathbf{r}_m$, $\mathbf{r}_s$, $\mathbf{r}_x$, $\mathbf{r}_d$ of vertices of the neutron path on the spectrometer surfaces. We will carry as much generality as possible.

The vector distances between vertices in the neutron path through the instrument are

$$\begin{aligned} \boldsymbol{\ell}_{ms} &= \mathbf{r}_s - \mathbf{r}_m \\ \boldsymbol{\ell}_{sx} &= \mathbf{r}_x - \mathbf{r}_s \\ \boldsymbol{\ell}_{xd} &= \mathbf{r}_d - \mathbf{r}_x\,. \end{aligned} \tag{38}$$

We define the mean positions of the elements of the instrument as

$$\begin{aligned} \mathbf{R}_m &= \langle \mathbf{r}_m \rangle = \frac{1}{A_m} \int_{A_m} \mathbf{r}_m\, d^2\mathbf{r}_m \\ \mathbf{R}_s &= \langle \mathbf{r}_s \rangle = \frac{1}{A_s} \int_{A_s} \mathbf{r}_s\, d^2\mathbf{r}_s \\ \mathbf{R}_x &= \langle \mathbf{r}_x \rangle = \frac{1}{A_x} \int_{A_x} \mathbf{r}_x\, d^2\mathbf{r}_x \\ \mathbf{R}_d &= \langle \mathbf{r}_d \rangle = \frac{1}{A_d} \int_{A_d} \mathbf{r}_d\, d^2\mathbf{r}_d\,, \end{aligned} \tag{39}$$

where the A s are areas of the relevant surfaces. The mean distances vectors between elements of the instrument are

$$\begin{aligned} \mathbf{L}_{ms} &= \mathbf{R}_s - \mathbf{R}_m \\ \mathbf{L}_{sx} &= \mathbf{R}_x - \mathbf{R}_s \\ \mathbf{L}_{xd} &= \mathbf{R}_d - \mathbf{R}_x\,. \end{aligned} \tag{40}$$

Nominal scattering angles follow from their cosines: the cosine of the nominal scattering angle at the sample is

$$\cos\varphi_{so} = \hat{L}_{ms}\cdot\hat{L}_{sx} = \frac{L_{ms}\cdot L_{sx}}{|L_{ms}||L_{sx}|} \tag{41}$$

and the cosine of the scattering angle at the analyzer (twice the nominal Bragg angle) is

$$\cos 2\theta_o = \hat{L}_{sx}\cdot\hat{L}_{xd} = \frac{L_{sx}\cdot L_{xd}}{|L_{sx}||L_{xd}|}. \tag{42}$$

Deviations of points on the vertices of the path through the instrument from the mean points are

$$\begin{aligned}\delta_m &= r_m - R_m\\ \delta_s &= r_s - R_s\\ \delta_x &= r_x - R_x\\ \delta_d &= r_d - R_d,\end{aligned} \tag{43}$$

as illustrated in Figure 4. Vector distances between points on the neutron trajectory are

$$\begin{aligned}\ell_{ms} &= R_s - R_m + \delta_s - \delta_m = L_{ms} + \delta_s - \delta_m\\ \ell_{sx} &= R_x - R_s + \delta_x - \delta_s = L_{sx} + \delta_x - \delta_s\\ \ell_{xd} &= R_d - R_x + \delta_d - \delta_x = L_{xd} + \delta_d - \delta_x\end{aligned} \tag{44}$$

and detailed scattering angles on the neutron path are

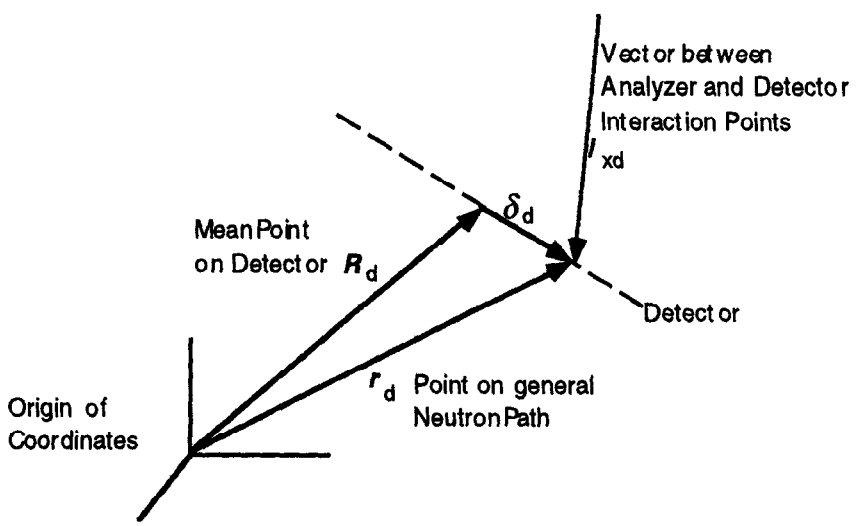

Figure 4. Illustration of the definition of position deviations on (for example) the detector surface.

$$\cos\varphi_s = \hat{\ell}_{ms}\cdot\hat{\ell}_{sx} = \frac{\ell_{ms}\cdot\ell_{sx}}{|\ell_{ms}||\ell_{sx}|} \tag{45}$$

and

$$\cos 2\theta = \hat{\ell}_{sx} \cdot \hat{\ell}_{xd} = \frac{\ell_{sx} \cdot \ell_{xd}}{|\ell_{sx}||\ell_{xd}|}, \tag{46}$$

in which the angles depend on the path through the instrument, that is, on r_m, r_s, r_x, r_d or, equivalently, on the deviations of the positions of the vertices from those of the nominal path through the instrument, δ_m, δ_s, δ_x, δ_d.

Now we work out expressions for various needed quantities as first-order approximations in the position deviations. The (scalar) length of the path between the emission point on the moderator to the scattering point on the sample is, for example,

$$\ell_{ms} = |\ell_{ms}| = (\ell_{ms} \cdot \ell_{ms})^{1/2} \tag{47}$$

so that

$$\ell_{ms} = [L_{ms}^2 + 2L_{ms} \cdot (\delta_s - \delta_m) + (\delta_s - \delta_m)^2]^{1/2}, \tag{48}$$

which to first order in the deviations is

$$\ell_{ms} \approx L_{ms}[1 + \hat{L}_{ms} \cdot (\delta_s - \delta_m) / L_{ms}],$$

thus also

$$\ell_{sx} \approx L_{sx}[1 + \hat{L}_{sx} \cdot (\delta_x - \delta_s) / L_{sx}]$$

and

$$\ell_{xd} \approx L_{xd}[1 + \hat{L}_{xd} \cdot (\delta_d - \delta_x) / L_{xd}]. \tag{49}$$

Similarly, the inverse flight path lengths, to first order, are

$$\frac{1}{\ell_{ms}} \approx \frac{1}{L_{ms}}[1 - \hat{L}_{ms} \cdot (\delta_s - \delta_m) / L_{ms}],$$

$$\frac{1}{\ell_{sx}} \approx \frac{1}{L_{sx}}[1 - \hat{L}_{sx} \cdot (\delta_x - \delta_s) / L_{sx}]$$

and

$$\frac{1}{\ell_{xd}} \approx \frac{1}{L_{xd}}[1 - \hat{L}_{xd} \cdot (\delta_d - \delta_x) / L_{xd}]. \tag{50}$$

The cosine of the scattering angle at the analyzer crystal is

$$\cos 2\theta = \hat{\ell}_{sx} \cdot \hat{\ell}_{xd} = \frac{\ell_{sx} \cdot \ell_{xd}}{\ell_{sx} \ell_{xd}} =$$

$$= \frac{1}{L_{sx} L_{xd}}[1 - \hat{L}_{sx} \cdot (\delta_x - \delta_s) / L_{sx}][1 - \hat{L}_{xd} \cdot (\delta_d - \delta_x) / L_{xd}](L_{sx} + \delta_x - \delta_s) \cdot (L_{xd} + \delta_d - \delta_x), \tag{51}$$

which to first order in the deviations is

$$\cos 2\theta = (\hat{L}_{sx} \cdot \hat{L}_{xd}) - (\hat{L}_{sx} \cdot \hat{L}_{xd})[\hat{L}_{sx} \cdot (\delta_x - \delta_s) / L_{sx} + \hat{L}_{xd} \cdot (\delta_d - \delta_x) / L_{xd}] +$$

$$+ \hat{L}_{sx} \cdot (\delta_d - \delta_x) / L_{xd} + \hat{L}_{xd} \cdot (\delta_x - \delta_s) / L_{sx}. \tag{52}$$

In (52), we recognize the leading term as the cosine of the nominal scattering angle at the analyzer,

$$\cos 2\theta_o = (\hat{L}_{sx} \cdot \hat{L}_{xd}) , \tag{53}$$

with the deviation of $\cos 2\theta$ from its nominal value

$$\delta(\cos 2\theta) = -\cos 2\theta_o [\hat{L}_{sx} \cdot (\boldsymbol{\delta}_x - \boldsymbol{\delta}_s)/L_{sx} + \hat{L}_{xd} \cdot (\boldsymbol{\delta}_d - \boldsymbol{\delta}_x)/L_{xd}] +$$

$$+ \hat{L}_{sx} \cdot (\boldsymbol{\delta}_d - \boldsymbol{\delta}_x)/L_{xd} + \hat{L}_{xd} \cdot (\boldsymbol{\delta}_x - \boldsymbol{\delta}_s)/L_{sx} . \tag{54}$$

The result for the cosine of the scattering angle at the sample is similar to (51) (replace s with m, replace x with s, replace d with x). With the assumed nondispersive (ε independent of the scattering vector) scattering at the sample, we have no explicit use for this. However, in the case of dispersive scattering, the analysis would require it, and would need to be redone with greater generality. We do not provide the result here.

Several tasks remain before the results become explicitly useful: to combine all these results into a first-order expression for the time-of-flight, to collect separately the coefficients of the deviations δ_m, δ_s, δ_x, δ_d; and to set explicit coordinate systems to represent the distributions F_m, F_s, F_x, and F_d. Focusing conditions will appear after the second of these steps is completed, in that the focusing conditions require that the collected coefficients are zero. The expression for the resolution will be explicit after the third step. Finally, representations for the Fs and for the reflectivity function $p_x(\lambda,\boldsymbol{q})$ are required to complete the calculation for the resolution width σ_g^2.

6. FOCUSING

We recall the expression for the time of arrival in terms of the deviations of the flight path lengths from their mean values and of the cosine of the analyzer scattering angle from its mean value

$$t = t_o + \frac{1}{v_o}[(\lambda'_o/\lambda_o)\delta\ell_1 + (\delta\ell_2 + \delta\ell_3)] - \frac{1}{4v_o}[(\lambda'_o/\lambda_o)^3 L_1 + (L_2 + L_3)] \frac{1}{\sin^2\theta_o}\delta(\cos 2\theta)$$

(25)

and introduce the somewhat simplified notation

$$L_1 = L_{ms} , \ \ell_1 = \ell_{ms} , \ \delta\ell_1 = \hat{L}_{ms} \cdot (\boldsymbol{\delta}_s - \boldsymbol{\delta}_m) , \tag{55}$$

$$L_2 = L_{sx} , \ \ell_2 = \ell_{sx} , \ \delta\ell_2 = \hat{L}_{sx} \cdot (\boldsymbol{\delta}_x - \boldsymbol{\delta}_s) , \tag{56}$$

$$L_3 = L_{xd} , \ \ell_3 = \ell_{xd} , \ \delta\ell_3 = \hat{L}_{xd} \cdot (\boldsymbol{\delta}_d - \boldsymbol{\delta}_x) . \tag{57}$$

We now collect terms that represent independently distributed contributions to the distribution of times of arrival:

$$t = t_o + (\boldsymbol{\delta}_m \text{ term}) + (\boldsymbol{\delta}_s \text{ term}) + (\boldsymbol{\delta}_x \text{ term}) + (\boldsymbol{\delta}_d \text{ term}) . \tag{58}$$

When these terms are made to vanish by choice of geometric parameters of the instrument, the corresponding contributions to the resolution width vanish.

The expression (25), correct though it is to first order in the deviations, does not imply that the variance of the time distribution, as, for example, in (37), is the sum of variances of those terms

separately. This is because the crystal reflection probability correlates the δ_s, δ_x, and δ_d distributions. Similar correlations would enter if collimators were included between elements of the instrument and treated in the analysis, which have not been included but could be. Nevertheless, if the terms in (58) are made to vanish by choice of geometric parameters, the corresponding contributions to the resolution vanishes and focusing is accomplished.

The δ_m term is

$$(\boldsymbol{\delta}_m \, term) = -\frac{1}{v_o}(\lambda'_o/\lambda_o)\hat{L}_1 \cdot \boldsymbol{\delta}_m \, . \tag{59}$$

Since δ_m is a vector that lies in the moderator surface, focusing clearly requires that the incident beam emerge perpendicularly from the moderator face; then the δ_m term is zero, independent of the extent of the moderator surface. This result may be intuitively obvious, but it is reassuring that it emerges from the present analysis.

The δ_s term is

$$(\boldsymbol{\delta}_s \, term) = \frac{1}{v_o}\{[(\lambda'_o/\lambda_o)\,\hat{L}_1 - \hat{L}_2] - \frac{1}{4sin^2\,\theta_o}[(\lambda'_o/\lambda_o)^3 L_1 + L_2 + L_3]\times$$

$$\times[cos\,2\theta_o \hat{L}_2/L_2 - \hat{L}_3/L_2]\} \cdot \boldsymbol{\delta}_s \tag{60}$$

The geometric implications of this term are not clear at this point; we leave it for further interpretation at a later stage of the analysis.

The δ_x term is

$$(\boldsymbol{\delta}_x \, term) = \frac{1}{v_o}\{(\hat{L}_2 - \hat{L}_3) - \frac{1}{4sin^2\,\theta_o}[(\lambda'_o/\lambda_o)^3 L_1 + L_2 + L_3]\times$$

$$\times[-cos\,2\theta_o(\hat{L}_2/L_2 - \hat{L}_3/L_3) - \hat{L}_2/L_3 + \hat{L}_3/L_2]\} \cdot \boldsymbol{\delta}_x \tag{61}$$

and the δ_d term is

$$(\boldsymbol{\delta}_d \, term) = \frac{1}{v_o}\{\hat{L}_3 - \frac{1}{4sin^2\,\theta_o}[(\lambda'_o/\lambda_o)^3 L_1 + L_2 + L_3]\times$$

$$\times[-cos\,2\theta_o \hat{L}_3/L_3 + \hat{L}_2/L_3]\} \cdot \boldsymbol{\delta}_d \, , \tag{62}$$

both of which we also leave for interpretation at a later stage of the analysis. Already, however, we can provide a preliminary interpretation. The focusing conditions (59-62) are vector inner products. The expressions can be made zero either if the bracketed quantity, a three-dimensional vector, is perpendicular to the corresponding vector deviation δ (that is, collinear with the vector normal to the surface) or if the vector itself is one of zero length. It may be possible, in view of the presence of the factor (λ_o'/λ_o), to provide exact focusing independently of the value of the energy transfer ε, by separately zeroing and/or orthogonalizing the ε-dependent and ε-independent terms in (60-62). Otherwise, if exact focusing is impossible or inconvenient, adequate reduction of the resolution width may be accomplishable for a finite range of energy transfers by keeping the terms (60-62) small. We note that the length of the initial flight path, L_1, appears explicitly in (60-62) so that focusing and resolution considerations cannot be based solely on the geometry of the secondary spectrometer.

In application, it may be useful to recall that the detector elements can be made small using an area sensitive detector comprising small, independently-operating flat elements, and that the analyzer properties can be varied as a function of position on the analyzer, as in a curved array of flat crystals in which the crystal cut and orientation may vary from one position to another. In addition, there may be cases where the sample is small and the corresponding contribution to the resolution, equation (60), is negligible. Then zeroing equation (60) may be superfluous and the remaining conditions for "partial focusing" may be easier to implement.

Equations (59-62) define elements of surfaces, "focused loci", in general curved, such that variations of position on those surfaces do not affect the time of arrival. They are the first order terms in a vector Taylor expansion of the time of arrival in terms of the local (planar) deviations of the positions from the mean positions of the elements of the spectrometer, equivalent respectively to

$$(\boldsymbol{r}_m - \boldsymbol{R}_m) \cdot \nabla_{\boldsymbol{r}_m} t(\boldsymbol{r}_m \boldsymbol{r}_s \boldsymbol{r}_x \boldsymbol{r}_d)\Big|_{\boldsymbol{R}_m \boldsymbol{R}_s \boldsymbol{R}_x \boldsymbol{R}_d} \tag{63}$$

$$(\boldsymbol{r}_s - \boldsymbol{R}_s) \cdot \nabla_{\boldsymbol{r}_s} t(\boldsymbol{r}_m \boldsymbol{r}_s \boldsymbol{r}_x \boldsymbol{r}_d)\Big|_{\boldsymbol{R}_m \boldsymbol{R}_s \boldsymbol{R}_x \boldsymbol{R}_d} \tag{64}$$

$$(\boldsymbol{r}_x - \boldsymbol{R}_x) \cdot \nabla_{\boldsymbol{r}_x} t(\boldsymbol{r}_m \boldsymbol{r}_s \boldsymbol{r}_x \boldsymbol{r}_d)\Big|_{\boldsymbol{R}_m \boldsymbol{R}_s \boldsymbol{R}_x \boldsymbol{R}_d} \tag{65}$$

$$(\boldsymbol{r}_d - \boldsymbol{R}_d) \cdot \nabla_{\boldsymbol{r}_d} t(\boldsymbol{r}_m \boldsymbol{r}_s \boldsymbol{r}_x \boldsymbol{r}_d)\Big|_{\boldsymbol{R}_m \boldsymbol{R}_s \boldsymbol{R}_x \boldsymbol{R}_d}, \tag{66}$$

although we have derived them by developing first order expansions rather than by calculating gradients. The general curved focused surfaces are defined by the exact equation

$$t(\boldsymbol{r}_m, \boldsymbol{r}_s, \boldsymbol{r}_x, \boldsymbol{r}_d) = \text{constant} = t(\boldsymbol{R}_m, \boldsymbol{R}_s, \boldsymbol{R}_x, \boldsymbol{R}_d), \tag{67}$$

to which the Taylor expansion is an approximation. Designs based on this linearized focusing analysis, whereby high resolution instrument configurations can be recognized in the analytical forms, need to be checked out, for example, by numerical integration of equation (35) or by Monte Carlo simulation, or by measurements in prototype arrangements.

We have finished our task at a preliminary level at which focusing conditions appear. It remains to introduce explicit geometric representations of the elements of the spectrometer in order to interpret the results and generate estimates of the resolution for non-focused conditions.

7. A NOTE ON THE INSPIRATION FOR THIS ANALYSIS

The inspiration for this analysis is the experience with powder and single-crystal diffraction, wherein it is possible to nullify the geometric instrumental resolution, at least for certain restricted conditions, and in resonance-detector/filter spectrometers. In the first case, the simple algorithm "$L \sin \theta$ = constant" [1] provides conditions on the orientation of source, sample, and detectors that allow use of large apertures and areas and the consequent intensity improvements while preserving q resolution. This focusing also provides data systems simplifications in time-of-flight powder diffraction instruments. Modern powder diffractometers accomplish this electronically. The single-crystal implementation has application in measurements of moderator emission time distributions [2] wherein the requirement is that the instrument contribution to the observed width be negligible within very tight constraints while the intensity is maintained at a useful level. These are "two-leg" instruments. Several crystal analyzer instruments ("three-leg" instruments) employ what might be called "partial focusing," QENS and CHEX at IPNS, TFXA and TOSCA at ISIS, and CAT and the LAM instruments at KENS. However, their designs may not have accounted for the full range of

effects treated here. Meanwhile, the high-resolution crystal analyzer instruments, LAM 80ET at KENS, and IRIS and OSIRIS at ISIS, employ nearly backscattering geometries that possibly can be made more general. In the case of the resonance spectrometers [3,4] (for deep inelastic, i.e. recoil, scattering) the same general ideas also work to improve the resolution.

ACKNOWLEDGMENT

I express my gratitude for the hospitality of the Rutherford Appleton Laboratory, where the opportunity for concentrated attention to this work made its accomplishment possible. I also thank E. B. Iverson and D. F. R. Mildner for assistance in checking the results.

REFERENCES

[1.] J. M. Carpenter, "Extended Detectors in Neutron Time-of-Flight Experiments," *Nucl. Instr. and Meth.* 47, 179 (1967).
[2.] K. F Graham and J. M. Carpenter, "Pulsed Moderator Studies Using a Time-Focused Crystal Spectrometer," *Nucl. Instr. and Meth.* 85, 163 (1970).
[3.] J. M. Carpenter and N. Watanabe, "Time Focusing and Resolution in Resonance Detector Neutron Spectrometers," *Nucl. Instr. and Meth.* 213, Nos. 2,3, 311 (1983).
[4.] J. M. Carpenter, N. Watanabe, S. Ikeda, Y. Masuda and S. Sato, "A Resonance Detector Spectrometer at KENS," *Physica* 120B, 126 (1983).

Appendix
The Wavevector Change for Scattering at the Analyzer

In order to evaluate the intensity and resolution either numerically or analytically, we require specific forms which represent the distributions of accessible positions on the moderator, sample, analyzer, and detector, and an explicit form for the reflection probability. In addition, for the same purposes, we need the expression for the unit reflection vector $\hat{\boldsymbol{q}}$, which we have not worked out above. For convenience in some of the envisioned uses, we represent this in terms of an expansion to first order in the flight path length deviations.

First, we develop a linearized expression for the unit vector $\hat{\boldsymbol{b}}$ that corresponds to a vector $\boldsymbol{b}$ which is itself the sum of two vectors, one large, $\boldsymbol{B}$, and one small, $\boldsymbol{\delta}$,

$$\boldsymbol{b} = \boldsymbol{B} + \boldsymbol{\delta} \; . \tag{A1}$$

The unit vector is

$$\hat{\boldsymbol{b}} = (\boldsymbol{B} + \boldsymbol{\delta}) / \left| \boldsymbol{B} + \boldsymbol{\delta} \right| . \tag{A2}$$

The inverse magnitude of the vector, to first order in the small quantity, is

$$1 / \left| \boldsymbol{B} + \boldsymbol{\delta} \right| \approx [B^2 + 2\boldsymbol{B} \cdot \boldsymbol{\delta}]^{-1/2} \approx B^{-1}[1 - \hat{\boldsymbol{B}} \cdot \boldsymbol{\delta} / B] \tag{A3}$$

where $\hat{\boldsymbol{B}}$ is the unit vector and B the magnitude of $\boldsymbol{B}$,

$$\hat{\boldsymbol{B}} = \boldsymbol{B} / B \tag{A4}$$

and

$$B = \left| \boldsymbol{B} \right| . \tag{A5}$$

Thus, to first order in $\boldsymbol{\delta}$,

$$\hat{\boldsymbol{b}} \approx \frac{1}{B}(\boldsymbol{B} + \boldsymbol{\delta})[1 - \hat{\boldsymbol{B}} \cdot \boldsymbol{\delta} / B] \approx \hat{\boldsymbol{B}} + \boldsymbol{\delta} / B - \hat{\boldsymbol{B}}(\hat{\boldsymbol{B}} \cdot \boldsymbol{\delta} / B) \; , \tag{A6}$$

which, to first order in $\boldsymbol{\delta}$, is manifestly a unit vector.

Because the scattering is elastic and the incident and scattered wavevectors are parallel to the vectors representing the incident and scattered paths to and from the analyzer, the direction of the wavevector change upon scattering at the analyzer is the same as the direction of the vector $\boldsymbol{q}$

$$\boldsymbol{q} = \hat{\boldsymbol{\ell}}_3 - \hat{\boldsymbol{\ell}}_2 \; , \tag{A7}$$

where the $\hat{\boldsymbol{\ell}}$ s are <u>unit</u> vectors in the directions of incidence and emergence from the analyzer. In terms of deviations from the means, the connecting <u>distance</u> vectors (44) are of the form

$$\boldsymbol{\ell} = \boldsymbol{L} + \delta\boldsymbol{\ell} \tag{A8}$$

so that for each, according to (A6), the unit vector $\hat{\boldsymbol{\ell}}$ is

$$\hat{\boldsymbol{\ell}} = \hat{\boldsymbol{L}} + \delta\boldsymbol{\ell} / L - \hat{\boldsymbol{L}}(\hat{\boldsymbol{L}} \cdot \delta\boldsymbol{\ell} / L) \; . \tag{A9}$$

Now we express the wavevector q in the form

$$q = q_o + \delta q \ , \tag{A10}$$

where

$$q_o = (\hat{L}_3 - \hat{L}_2) \tag{A11}$$

and

$$\delta q = \frac{\delta \ell_3}{L_3} - \frac{\delta \ell_2}{L_2} - \hat{L}_3(\hat{L}_3 \cdot \frac{\delta \ell_3}{L_3}) + \hat{L}_2(\hat{L}_2 \cdot \frac{\delta \ell_2}{L_2}) \ . \tag{A12}$$

By (A6) we find

$$\hat{q} = \hat{q}_o + \frac{\delta q}{\left|\hat{L}_3 - \hat{L}_2\right|} - \hat{q}_o \frac{\hat{q}_o \cdot \delta q}{\left|\hat{L}_3 - \hat{L}_2\right|} \ . \tag{A13}$$

The leading term in (A13) is the unit vector corresponding to the geometrically definednominal scattering vector at the analyzer, $\hat{q}_o$,

$$\hat{q}_o = \frac{(\hat{L}_3 - \hat{L}_2)}{\left|\hat{L}_3 - \hat{L}_2\right|} \ . \tag{A14}$$

Here,

$$\left|\hat{L}_3 - \hat{L}_2\right|^2 = 2\,(1 - \hat{L}_3 \cdot \hat{L}_2) = 2(\,1 - cos\,2\theta_o\,) = 4sin^2\theta_o \ , \tag{A15}$$

so that

$$\left|\hat{L}_3 - \hat{L}_2\right| = 2sin\theta_o \ . \tag{A16}$$

Now writing

$$\hat{q} = \hat{q}_o + \delta\hat{q} \ , \tag{A17}$$

we find from (A13), after some arithmetic, that $\delta\hat{q}$ is

$$\delta\hat{q} = \frac{1}{2\ sin\ \theta_o}\left\{ \begin{array}{l} \dfrac{\delta \ell_3}{L_3} - \dfrac{\delta \ell_2}{L_2} + \dfrac{1}{2}(\hat{L}_2 + \hat{L}_3)(\hat{L}_2 \cdot \dfrac{\delta \ell_2}{L_2} - \hat{L}_3 \cdot \dfrac{\delta \ell_3}{L_3}) - \\ \\ \qquad - \dfrac{1}{4sin^2\ \theta_o}(\hat{L}_2 - \hat{L}_3)(\hat{L}_2 - \hat{L}_3) \cdot (\dfrac{\delta \ell_3}{L_3} - \dfrac{\delta \ell_2}{L_2}) \end{array} \right\} \ , \tag{A18}$$

in which

$$\delta \ell_2 = \delta_x - \delta_s \tag{A19}$$

and

$$\delta \ell_3 = \delta_d - \delta_x \ . \tag{A20}$$

It is probably as well in practice to use (A14) and (A16) with δq from (A12) recursively to compute $\hat{q}$ and $\delta\hat{q}$ in (A13).